Phase Equilibria in Mixtures of Polar and Nonpolar Compounds

Derived Thermodynamic Quantities for Alcohols and Hydrocarbons

CLINE BLACK
Shell Development Company, Emeryville, California

The properties of vapor mixtures and liquid solutions which determine phase equilibria are of special importance in separation processes. They include the vapor-phase imperfections; the liquid-phase activity coefficients; and the excess heat, entropy, and free energy of mixing.

Correlation of these properties in nonpolar mixtures is relatively simple, but in mixtures of polar and nonpolar compounds the molecular interactions lead to more complex relations. Semiempirical relations reported earlier (*3*, *4*) have been used to calculate the vapor imperfections and to correlate the liquid-phase activity coefficients.

Temperature variations of the activity coefficients can reflect the true heat and entropy effects in solution if sufficient vapor-liquid equilibria are available for a careful and consistent treatment. This is illustrated with binary mixtures of benzene and the *n*-aliphatic alcohols, methanol to pentanol. The results are compared with calorimetric data available in the literature.

The consistent set of cross-correlated coefficients provides a basis for calculating both isothermal and isobaric vapor-liquid equilibria at various conditions for the binaries and for certain ternary and multicomponent mixtures without any additional data.

Most industrial petroleum and chemical processes involve separations in which the products of interest are separated from the undesirable components. Many of these separation schemes depend directly or indirectly on the phase equilibria in the mixtures. Consequently the properties of vapor mixtures and liquid solutions which determine the phase equilibria are of special importance. These include the vapor-phase imperfections; the liquid-phase activity coefficients; and the excess heat, entropy, and free energy of mixing.

Correlation of these properties in nonpolar mixtures is relatively simple, but molecular interactions in mixtures of polar and nonpolar compounds are more complex and lead to more involved algebraic relations.

Even though the excess free energy of mixing does not appear highly sensitive to change in temperature, the heat of mixing depends directly on these changes. Correlations which incorporate temperature variations of the activity coefficients can reflect the true heat and entropy effects in solution if sufficient vapor-liquid equilibria are available for a careful and consistent treatment. This is illustrated with binary mixtures of benzene and the *n*-aliphatic alcohols, methanol to *n*-pentanol. These represent some of the more complex cases, as interassociation between unlike molecules as well as dissociation of the alcohol polymers takes place upon mixing.

From the cross-correlated results both isothermal and isobaric equilibria can be predicted at any prescribed condition in the range of the correlations. This is illustrated for ten alcohol-hydrocarbon binaries and for some ternary and multicomponent mixtures of the components. The more extensive tabulations are available through the American Documentation Institute.*

CORRELATION OF VAPOR-LIQUID EQUILIBRIA

Complete vapor-liquid equilibria provide the relation between the liquid composition, the vapor composition, and the total pressure or boiling temperature of the solution. It is conventional to correlate such data through the activity coefficients in the liquid and the imperfections in the vapors.

Activity coefficients have been calculated from vapor-liquid equilibria according to

$$\log \gamma_i = \log (Y_i P / x_i P_i^0) + \log \theta_i \quad (1)$$

The latter includes the influences of both vapor imperfections and pressure on the liquid phase.

These coefficients were derived from a special approximation (*3*) in which the nonpolar and polar parts of the energies of attraction of the pure components are combined separately for representing mixtures. If b_i and a_i are van der Waals' covolume and cohesive energy constants,

---

*Tabular material has been deposited as document 5912 with the American Documentation Institute, Photoduplication Service, Library of Congress, Washington 25, D. C., and may be obtained for $2.50 for photoprints or $1.75 for 35-mm. microfilm.

TABLE 1. CONSTANTS FOR POLAR AND NONPOLAR COMPOUNDS

	T_c, °K.	$P_{c,atm.}$	E'	m	χ
Methanol	513.3	78.7	0.120	4.75	51.2
Ethanol	516.3	63.1	0.089	4.75	75.9
Isopropanol	508.2	53.0	0.080	4.75	95.2
n-Propanol	536.88	50.0	0.080	4.75	96.17
n-Butanol	560.0	48.4	0.075	4.75	119.61
n-Pentanol	586.1	44.0	0.072	4.75	143.4
Benzene	561.66	47.7	0	—	116.1
Toluene	594.0	41.6	0	—	141.7
Methylcyclohexane	571.1	34.5	0	—	167.9
n-Heptane	540.2	27.0	0	—	189.0

TABLE 2. COEFFICIENTS FOR THE MODIFIED VAN LAAR-TYPE OF EQUATIONS ALCOHOL-BENZENE SYSTEMS

t, °C.	A_{12}	A_{21}	c_{12}	Type of data	Source of original data
Methanol-benzene					
20	1.1900	0.8950	0.1470	Isothermal	*(20)*
35	1.1304	0.8713	0.1320	Isothermal	*(24)*
40	1.1083	0.8623	0.1262	Isothermal	*(19)*
55	1.0400	0.8350	0.1090	Isothermal	*(24)*
(59)	1.0226	0.8275	0.1050	Isobaric	*(33)*
Ethanol-benzene					
20	1.0700	0.7715	0.1142	Constant pressure data	*(21)*
45	0.9800	0.7250	0.0980	Isothermal	*(6)*
(68)	0.9015	0.6870	0.0831	Isobaric, 760 mm. Hg	*(8)*, *(31)*
Isopropanol-benzene					
25	0.9370	0.6670	0.0841	Isothermal	*(22)*
n-Propanol-benzene					
(27.8)	0.9290	0.6610	0.0832	Isobaric, 100 mm. Hg	*(5)*
40	0.8930	0.6370	0.0785	Isothermal	*(19)*
(48.8)	0.8680	0.6200	0.0754	Isobaric, 275 mm. Hg	*(5)*
(76.1)	0.7980	0.5740	0.0659	Isobaric, 750 and 760 mm. Hg	*(31)*, *(5)*
n-Butanol-benzene					
25	0.8155	0.5550	0.0625	Isothermal	*(1)*
(83.6)	0.6950	0.4500	0.0500	Isobaric, 760 mm. Hg	*(32)*
n-Pentanol-benzene					
(89)	0.5850	0.3305	0.0340	Isobaric, 760 mm. Hg	*(32)*

TABLE 3. COEFFICIENTS FOR THE MODIFIED VAN LAAR EQUATIONS ALCOHOL-TOLUENE SYSTEMS

t, °C.	A_{12}	A_{21}	c_{12}	Type of data	Reference
Methanol-toluene					
(64.44)	0.9700	0.9290	0.1000	Isobaric, 760 mm. Hg	*(2)*
Ethanol-toluene					
t, °C.	A_{12}	A_{21}	c_{12}		
35	1.0620	0.7990	0.1048	Isothermal	*(15)*
55	0.9880	0.7630	0.0911	Isothermal	*(15)*

TABLE 4. COEFFICIENTS FOR THE MODIFIED VAN LAAR EQUATIONS ETHANOL-SATURATED C_7 HYDROCARBONS

t, °C.	A_{12}	A_{21}	c_{12}	Type of data	Reference
Ethanol-methylcyclohexane					
35	1.205	1.060	0.185	Isothermal	*(16)*
55	1.140	1.010	0.165	Isothermal	*(16)*
Ethanol-*n*-heptane					
t, °C.	A_{12}	A_{21}	c_{12}	Type of data	Reference
30	1.271	1.238	0.280	Isothermal	*(28)*
(37.5)	1.242	1.206	0.264	Isobaric, 180 mm. Hg	*(14)*
50	1.200	1.154	0.240	Isothermal	*(28)*
(55)	1.184	1.136	0.230	Isobaric, 400 mm. Hg	*(14)*
70	1.138	1.081	0.205	Isothermal	*(28)*
				Isobaric, 750 mm. Hg	*(14)*

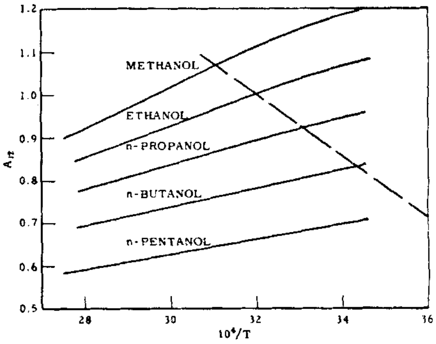

Fig. 1. Coefficient A_{12} in the modified van Laar equations—alcohols (1) with benzene (2).

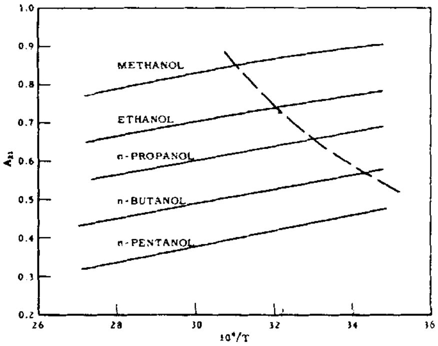

Fig. 2. Coefficient A_{21} in the modified van Laar equation—alcohols (1) with benzene (2).

respectively, the molal cohesive energy is represented by $a_i\xi_i^0$. It is assumed that the vapor mixtures can be predicted from the properties of the individual components. The corresponding rigorous expression for θ_i becomes

$$\log \theta_i = [(P - P_i^0)/2.3RT] \cdot [b_i - V_i' - a_i\xi_i^0/RT + (P/2\cdot 3R^2T^2)[(\sum G_{ij}Y_j)^2 + (\sum \bar{G}_{ij}Y_j)^2] \quad (2$$

For nonpolar compounds the attraction coefficients are predicted from the critical temperature and pressure. Polar compounds require individual coefficients which can be determined from a minimum of vapor-density data. Such coefficients have been given earlier *(3)* for methanol and ethanol. Coefficients for the higher alcohols have been estimated from the carbon number with the aid of the empirical equation

$$E' = 0.06 + 0.06/n_c \quad (3)$$

derived from available vapor-density data *(10, 11, 12, 17, 18, 23)* for the low-molecular-weight alcohols. These coefficients together with the critical constants are given in Table 1.

The constants χ_i given also in Table 1 are used to estimate the approximate molal-liquid volumes of the components in solution according to the empirical equation

$$V' = \chi/(1.70897 - 0.74575T_r - 0.26048T_r^5) \tag{4}$$

Since the contribution of V' in Equation (2) is relatively small, Equation (4) is an adequate approximation. As the temperature approaches the critical value, Equation (4) predicts molal volumes lower than those of the pure components. At low reduced temperatures the values are nearly the same.

The activity coefficients have been correlated as described earlier (*4*) with the aid of the two plots

$$(\log \gamma_1)^{0.5} \; vs. \; (\log \gamma_2)^{0.5} \tag{5}$$

and

$$\log (\gamma_1/\gamma_2) \; vs. \; x_i \tag{6}$$

The data have been represented with the aid of the modified van Laar type of equations (*4*), which for binary systems are given according to

$$\left.\begin{aligned} \log \gamma_1 &= a_{12}^2/(1 + a_{12}^2 x_1/a_{21}^2 x_2)^2 + E_1 \\ \log \gamma_2 &= a_{21}^2/(1 + a_{21}^2 x_2/a_{12}^2 x_1)^2 + E_2 \\ E_i &= c_{ij} x_j (x_i - x_j) \cdot [3(x_i - x_j)(1 - x_i) + 2x_j] \end{aligned}\right\} \tag{7}$$

A summary of the coefficients derived in this way for binary systems consisting of an alcohol and benzene are given in Table 2, together with the source of the experimental data used.

The influence of temperature on the coefficients is shown in Figures 1, 2, and 3, in which A_{12}, A_{21}, and c_{12} are plotted vs. the temperature. The coefficient A_{12} is the logarithm of the activity coefficient of component 1, the alcohol, at infinite dilution in liquid 2, benzene. The consistent change in A_{12} as the carbon number of the alcohol varies from 1 to 5 is evident in Figure 1. Similar consistent changes are noted in the logarithm of the activity coefficient of component 2 at infinite dilution A_{21} and in c_{12} in Figures 2 and 3, respectively.

Increasing the temperature causes a decrease in A_{12}, A_{21}, and c_{12}. The shape of the curves in Figures 1, 2, and 3 for methanol and benzene are quite well established from the isothermal data of Niini (*20*) at 20°C., of Scatchard and coworkers (*24, 26*) at 35° and 55°C. with single points at 25° and 45°C., and of Lee (*19*) at 40°C. and the isobaric data of Williams and coworkers (*33*).

Below about 50°C. for methanol-benzene, as noted in Figure 1, the curve of A_{12} vs. $1/T$ begins to deviate appreciably from a linear relation. With ethanol and benzene a similar curvature is noted below about 40°C., as indicated by the dashed line. For *n*-propanol this occurs at a still lower temperature, probably below about 30°C. This is undoubtedly due to an increased interassociation (*13*) between the alcohol and benzene as the temperature decreases. For alcohols with four or more carbons the data do not establish the shape of A_{12} vs. $1/T$ as well, but it appears from the available data that in the temperature region of 20° to 70°C. the relation is nearly linear and the molal heats of mixing at given composition are practically independent of temperature. These same observations and conclusions are evident also in Figures 2 and 3.

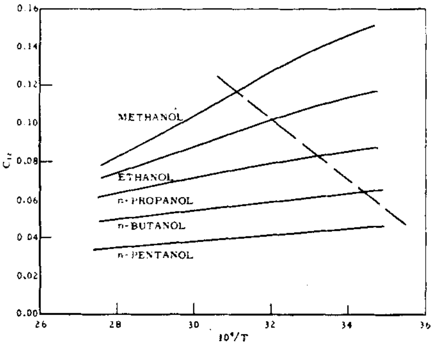

Fig. 3. Coefficient c_{12} in the modified van Laar equation—alcohols (1) with benzene (2).

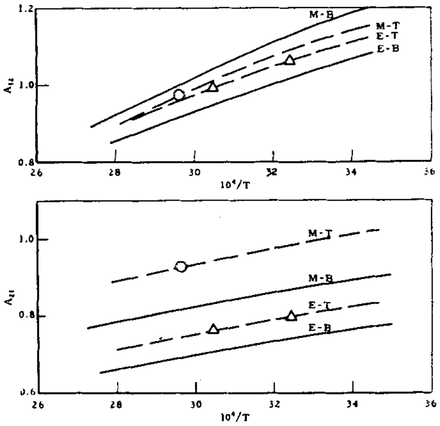

Fig. 4. Influence of temperature on A_{12} and A_{21} for methanol-toluene and ethanol-toluene, based on curves for methanol-benzene and ethanol-benzene.

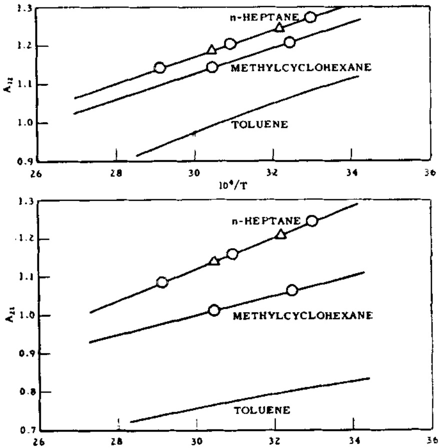

Fig. 5. Influence of hydrocarbon type on A_{12} and A_{21} ethanol (1) with hydrocarbons (2).

The coefficients A_{12}, A_{21}, and c_{12} decrease as the carbon number increases going from methanol to *n*-pentanol. A nearly linear change is noted if cross plots at constant temperature are prepared from Figures 1, 2, and 3. The coefficients for *n*-pentanol–benzene at temperatures below 89°C. were obtained from such cross plots.

Available vapor-liquid equilibrium data are not sufficient to establish the shape of the curves A_{12}, A_{21}, and c_{12} vs. $1/T$ for methanol and toluene. Indeed only the isobaric data at 760 mm. Hg are known (*2*), which help to establish the three coefficients near 64°C. For ethanol and toluene data at only 35 and 55°C. are known (*15*). But these two systems can be predicted from these meager data, Table 3, and the established curves for methanol-benzene and ethanol-benzene. As shown in Figure 4, the dashed curves for the toluene systems are drawn in through the data to have shapes similar to the corresponding benzene systems shown as full lines. This is nearly equivalent to the assumption of equal heats of mixing for the toluene and benzene systems with a given alcohol and will be discussed later.

The influence of hydrocarbon type on the coefficients A_{12}, A_{21}, and c_{12} is illustrated with the systems ethanol-methylcyclohexane and ethanol–*n*-heptane, which will be compared with ethanol-toluene. The coefficients derived for the modified van Laar type of equations and the data sources for these saturated hydrocarbons with ethanol are given in Table 4. The coefficients are given in Figures 5 and 6 for binary mixtures of ethanol in *n*-heptane, methylcyclohexane, and toluene.

EXCESS FREE ENERGIES, HEATS, AND ENTROPIES OF MIXING

The heat of mixing and the excess entropy of mixing have been calculated from the excess free energy of mixing and the variation of the activity coefficients with temperature at constant composition. The modified van Laar equations (*4*) for binary systems [Equations (7)] have been used to calculate log γ_i's at given compositions. The excess free energy per mole is calculated at any given composition according to

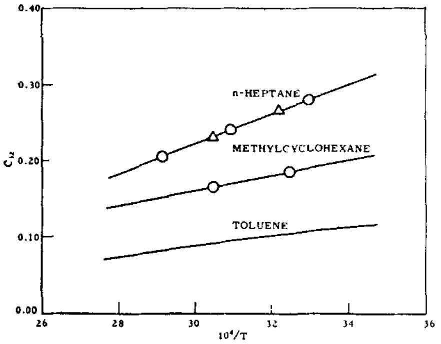

Fig. 6. Influence of hydrocarbon type on c_{12} ethanol with hydrocarbons.

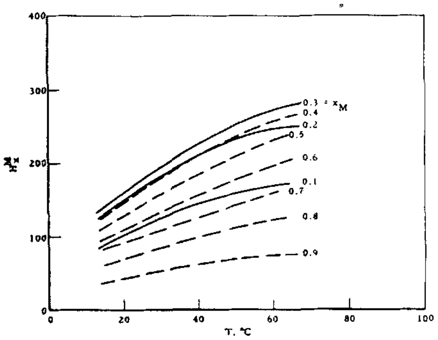

Fig. 7. Influence of temperature on H_x^M at constant composition methanol with benzene.

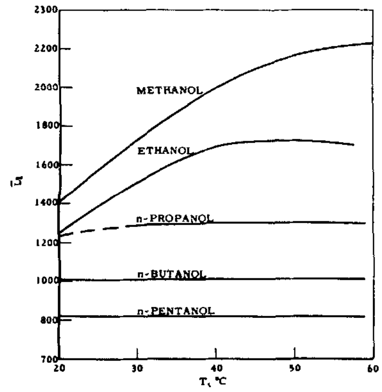

Fig. 8. Differential heat of mixing of alcohol at infinite dilution in benzene vs. temperature.

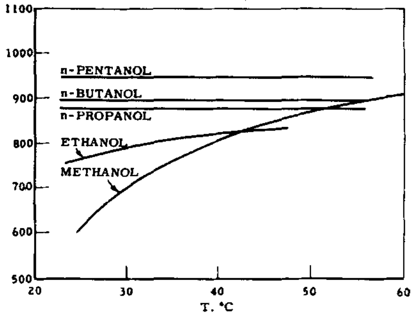

Fig. 9. Differential heat of mixing of benzene at infinite dilution in alcohols vs. temperature.

$$F_x^E = 2.303RT(\sum x_i \log \gamma_i)_x \qquad (8)$$

The differential heat of mixing per mole is calculated from the change of $\log \gamma_i$ with temperature at given composition with the aid of

$$\overline{L}_{i_x} = 2.303R(\Delta \log \gamma_i)_x/\Delta(1/T) \qquad (9)$$

and the integral heat of mixing per mole is calculated by

$$H_x^M = \sum x_i \overline{L}_{i_x} \qquad (10)$$

The temperature intervals have been selected so that the results reflect the proper rate of change in the nonlinear regions of $\log \gamma_i$ vs. $1/T$. The heats of mixing calculated for each temperature interval have been considered to correspond to the temperature of the average $1/T$'s.

The heats of mixing derived at constant composition at three different temperatures are plotted vs. temperature in Figure 7 for methanol-benzene mixtures. In the range of the data, 20° to 60°C., the heat of mixing increases as the temperature increases; it probably reaches a maximum at a somewhat higher temperature, and at a still higher temperature level it will probably decrease as the temperature is increased. This behavior is to be expected if the temperature coefficient of interassociation (*13*) between unlike molecules is sufficiently greater than the temperature coefficient of association of the methanol molecules. In addition to the ordinary heat effects resulting from nonpolar forces association gives rise to positive heat of mixing or heat absorbed, and interassociation results in negative heat of mixing or heat evolved.

Similar calculations have been made for methanol-toluene, ethanol-benzene, *n*-propanol–benzene, *n*-butanol–benzene, *n*-pentanol-benzene, ethanol-toluene, ethanol-methylcyclohexane, and ethanol–*n*-heptane. The differential heats of mixing at infinite dilution for each component are given in Table 5 for these systems. For the lower alcohols in mixtures with benzene or toluene the differential heat of mixing increases as the temperature increases in the range considered; for the higher alcohols the differential heats of mixing are practically independent of temperature.

In Figure 8 the differential heats of mixing for the alcohols at infinite dilution in benzene are plotted vs. temperature. As the carbon number increases, the differential heat of mixing of the alcohol at infinite dilution $\overline{L}_1$ decreases at a given temperature. For mixtures with methanol and ethanol the differential heat of mixing $\overline{L}_1$ increases as temperature increases, levels off, and probably goes through a very flat maximum. This is probably true with the higher alcohols, with the maximum occurring at successively lower temperatures.

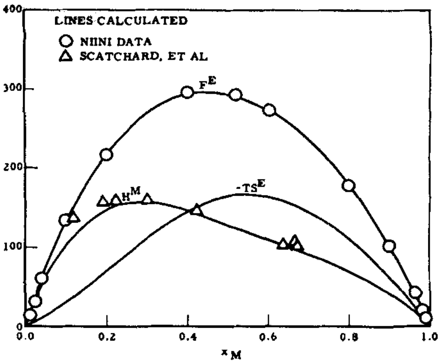

Fig. 10. Excess free energy, heat, and entropy of mixing, cal./g. mole methanol-benzene at 20°C.

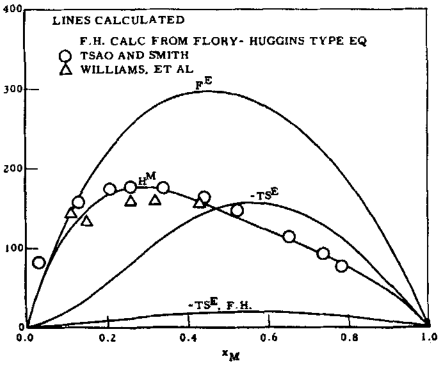

Fig. 11. Excess free energy, heat, and entropy of mixing, cal./g. mole methanol-benzene at 25°C.

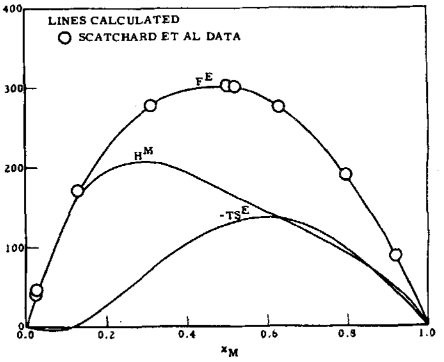

Fig. 12. Excess free energy, heat, and entropy of mixing, cal./g. mole methanol-benzene at 35°C.

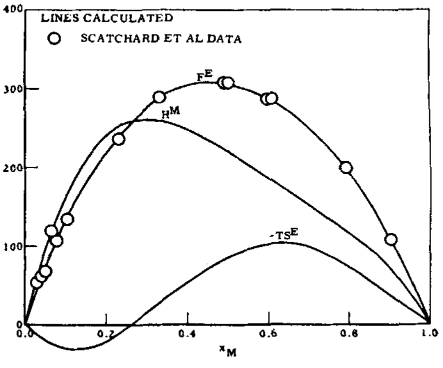

Fig. 13. Excess free energy, heat, and entropy of mixing, cal./g. mole methanol-benzene at 55°C.

The differential heat of mixing $\overline{L}_2$ for benzene at infinite dilution in the homologous series of alcohols from methanol to *n*-pentanol is plotted vs. temperature in Figure 9. In the low-temperature region the differential heat of mixing for benzene increases in going from methanol to *n*-pentanol. At a higher temperature level where interassociation has less influence this may not be entirely true.

Table 5. Differential Heats of Mixing at Infinite Dilution Derived from Vapor-Liquid Equilibria

System	*t*, °C.	$\bar{L}_1$	$\bar{L}_2$	
Methanol-benzene	27.3	1,642	653	
	44.7	2,091	840	
	62.3	2,233	921	
Ethanol-benzene	27.3	1,440	777	
	39.9	1,695	821	
	56.1	1,695	821	
Propanol-benzene	38	1,288	865	(Nearly constant 30° to 60°C.)
Butanol-benzene	50	1,000	872	(Nearly constant 20° to 60°C.)
Pentanol-benzene	36.5	817	943	(Nearly constant 20° to 60°C.)
Methanol-toluene	27.3	1,405	840	
	42.3	1,853	866	
	57.1	2,035	966	
Ethanol-toluene	27.3	1,441	799	
	44.7	1,712	833	
Ethanol-methylcyclohexane	55	1,504	1,157	
Ethanol-*n*-heptane	55	1,573	1,852	(Nearly constant 30° to 70°C.)

Table 6. Heats of Mixing for Methanol-Benzene

H^M, cal./g. mole at $x_m = 0.3$

t, °C.	From V-L equil.	Exptl.*	Reference for calorimetric data	
15	140	139	Schmidt	(*27*)
20	158	159	Scatchard, *et al.*	(*25*)
20	158	190–195	Wolfe, *et al.*	(*34*)
23	167	150	Washburn and Lightbody	(*30*)
25	176	156	Williams, *et al.*	(*33*)
25	176	175	Tsao and Smith	(*29*)

*Calorimetric data.

Table 7. Approximate Heats of Mixing for Binary Systems of Alcohols and Hydrocarbons Derived from Vapor-Liquid Equilibria

		H^M, cal./g. mole								
Systems	*T*, °C.	0.10	0.20	0.30	0.40	0.50	0.60	0.70	0.80	0.90*
Methanol-benzene	25	115	165	176	163	142	121	101	77	48
	55	164	242	262	248	220	186	151	118	71
Ethanol-benzene	25	105	165	189	191	181	163	138	107	62
	55	130	197	223	222	206	181	153	116	68
Propanol-benzene	55	105	170	206	219	216	200	172	131	75
Butanol-benzene	55	86	147	187	207	212	201	174	134	76
Pentanol-benzene	20 to 60	76		182		220		188		83
Methanol-toluene	25	108	155	174	173	163	145	122	92	55
	55	152	230	259	253	232		170	132	
Ethanol-toluene	25	107	167	193	196	188	171	145	110	63
	55	131	200	227	227	211	187	156	119	69
Ethanol-methylcyclohexane	55	117	180	208	216	212	200	180	147	92
Ethanol-*n*-heptane	55	116	171	193	202	208	215	216	197	136

*Column headings 0.10, 0.20. . . 0.90 refer to the mole fractions of alcohol in the liquid for each binary.

Table 8. Maximum Heats of Mixing

		Maximum H^M at any composition, cal./g. mole		
	t, °C.	From V-L equil.	Exptl.*	Reference
Ethanol-benzene	23	185	182	(*30*)
n-Propanol–benzene	20 to 60	219	—	
	15		232	(*27*)
n-Pentanol–benzene	20	220	223	(*7*)
Methanol-toluene	23	167	159	(*30*)
Ethanol-toluene	23	195	183	(*30*)

*Calorimetric

Integral heats of mixing taken from Figure 7 for methanol-benzene mixtures at a mole fraction of 0.3 for methanol are compared in Table 6 with calorimetric values reported by several investigators (*25*, *27*, *29*, *30*, *33*, *34*).

The results derived from vapor-liquid equilibrium data are in substantial agreement with the calorimetric measurements of Schmidt (*27*), Scatchard, *et al.* (*25*), and Tsao and Smith (*29*). The results of Williams, *et al.* (*33*), and of Washburn and Lightbody (*30*) are slightly lower than the derived values, and those of Wolfe, *et al.* (*34*), are somewhat higher than any of the others. No values were calculated at temperatures as low as 15°C., but an extrapolation to 15°C. in Figure 7 gives results in good agreement with those of Schmidt.

The excess entropy of mixing has been calculated from the excess free energy and the heat of mixing at fixed composition according to

$$-TS_x^E = F_x^E - H_x^M \qquad (11)$$

The three quantities at 20°C. are shown graphically in Figure 10 for mixtures of methanol and benzene. The excess free energy calculated from the data of Niini (*20*) are shown also. The calorimetric heats of mixing of Scatchard, *et al.* (*25*), are also compared with the derived results in Figure 10.

The three derived thermodynamic quantities F_x^E, H_x^M, and $-TS_x^E$ at 25°C. are plotted in Figure 11, where the heats of mixing are compared with the calorimetric data of Tsao and Smith (*29*) and Williams, Rosenberg, and Rothenberg (*7*) for methanol-benzene. Since the latter data were given graphically, only the points in the region of the maximum are shown for this source. The entropies predicted from the Flory-Huggins relation when applied to these mixtures are much too low. (See the curve marked F.H. in Figure 11.)

For mixtures of methanol and benzene the integral heat of mixing increases as temperature increases up to about 60° or 80°C. In the same region the excess free energy increases only slightly. The excess entropy of mixing is negative and changes to smaller negative values as the temperature increases. The three quantities F_x^E, H_x^M, and $-TS^E$ are given in Figures 12 and 13 for 35° and 55°C., respectively. At low concentrations of methanol the entropy has already become positive at 35°C. (Figure 12), and this positive region increases as temperature increases further (Figure 13).

Figure 14 shows values of F_x^E, H_x^M, and $-TS_x^E$ for methanol-toluene mixtures derived from the modified van Laar equations with coefficients represented by the curves in Figure 4. It will be remembered that only isobaric data at 760 mm. Hg were available to establish the coefficients at 64.44°C., and the temperature influence was obtained by drawing in the curves with shapes similar to the corresponding benzene systems. The calorimetric values for the heat of mixing of Tsao and Smith (*29*) are shown also in Figure 14.

Although the symmetry of the derived results is not in perfect agreement with the data, the magnitude of the values is about right. A comparison of Figures 14 and 11 shows both the maximum heat of mixing and the maximum excess entropy of mixing to be very nearly equal for toluene and benzene mixtures with methanol. The slightly different symmetry of the heat and entropy curves vs. x^M in the two systems furnishes a higher maximum in the excess free-energy curve for toluene. The data of Tsao and Smith show the heats of mixing for toluene and benzene in methanol to be practically the same at 25°C. The derived heats of mixing at 55°C. are a little higher for mixtures of toluene and methanol than for mixtures of benzene and methanol. These differences may not be real but may be only a reflection of the approximate nature of the slopes of the toluene-methanol curves as established in Figure 4.

Integral heats of mixing derived from the vapor-liquid equilibria and its variation with temperature are given in Table 7 for a few systems at one or two temperatures. For temperatures up to about 60° to 80°C. the heat of mixing of methanol and benzene increases as temperature increases. This limit appears to occur at successively lower temperatures as one goes from methanol to *n*-pentanol in the homologous series. For *n*-pentanol-benzene mixtures the limit is probably below 20°C.

The maximum heat of mixing at any composition has been plotted vs. temperature in Figure 15 for the five alcohols, methanol to *n*-pentanol, in mixtures with benzene. At low temperatures, for example at 25°C., the maximum heat of mixing increases as the carbon number of the alcohol increases. That butanol falls just below propanol and pentanol is not significant. Within the accuracy of the calculations the maximum H^M at any composition can be considered the same for benzene in *n*-propanol, *n*-butanol, and *n*-pentanol, but in ethanol and methanol the differences are significant.

The derived maximum heat of mixing at any composition is compared with available calorimetric data for five systems in Table 8. As with methanol-benzene mixtures in Table 6, the derived results for methanol-toluene are also slightly higher than the measured values of Washburn and Lightbody (*30*). Even so, the deviations of the derived from the experimental values are less than 7% for each of the systems.

The influence of hydrocarbon type on the three quantities F^E, H^M, and $-TS^E$ is shown in Figure 16 for mixtures of ethanol with *n*-heptane, methylcyclohexane, and toluene at 55°C. The excess free energy decreases in the order *n*-heptane, methylcyclohexane, toluene. The maximum heat of mixing at any composition is nearly the same for the three binaries, but the symmetry of the systems is different. It will be noted also that the maximum heat of mixing is about the same for these systems as for systems composed of benzene with any alcohol from ethanol to *n*-pentanol at the same temperature. Both the magnitude and the symmetry of the excess entropy of mixing vs. x_E are different for the three systems. The excess entropy is negative and decreases to smaller negative values going from heptane to methylcyclohexane to toluene at concentrations of ethanol less than about 60% mole. At low concentrations of ethanol TS^E becomes slightly positive in mixtures with toluene.

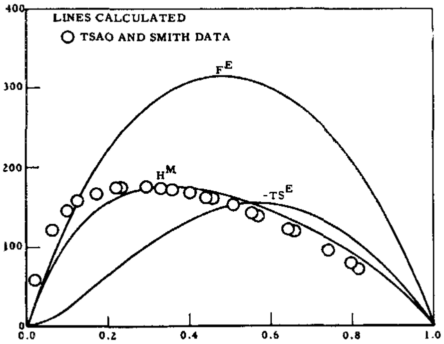

Fig. 14. Excess free energy, heat and entropy of mixing, cal./g. mole methanol-toluene at 25°C.

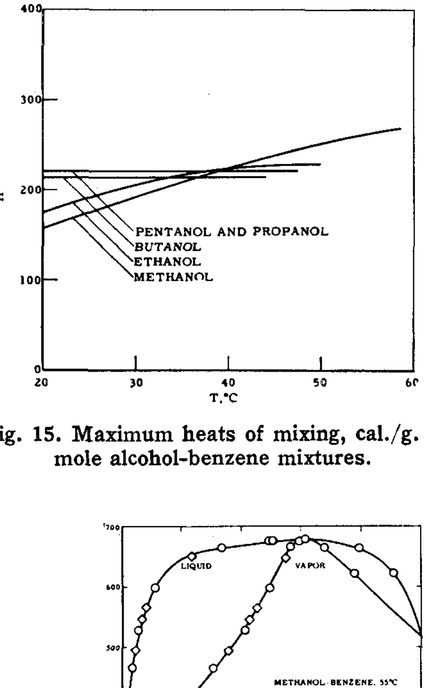

Fig. 15. Maximum heats of mixing, cal./g. mole alcohol-benzene mixtures.

DERIVED VAPOR-LIQUID EQUILIBRIA

Having correlated the activity coefficients as a function of composition and confirmed the validity of their temperature dependence by comparing calculated and observed heats of mixing, one can now use the cross-correlated coefficients to predict thermodynamically consistent sets of vapor-liquid equilibria. This has been done for both isothermal and isobaric conditions.

The procedure for isothermal calculations is to start with known liquid compositions, calculate the activity coeffi-

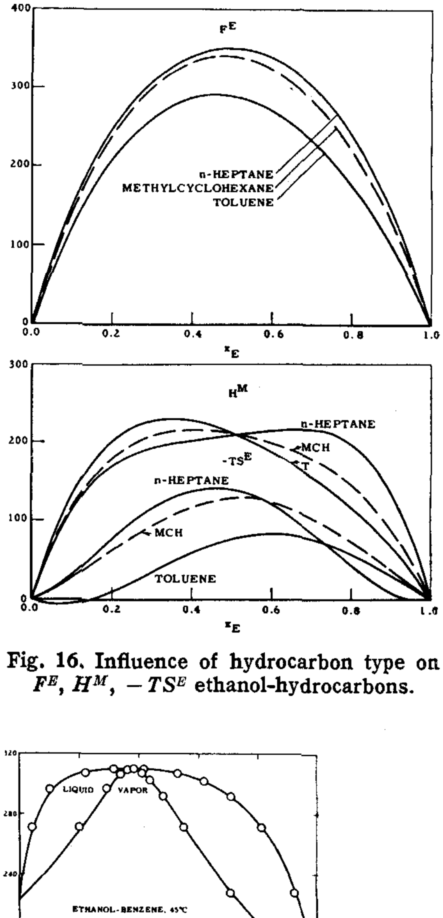

Fig. 16. Influence of hydrocarbon type on F^E, H^M, $-TS^E$ ethanol-hydrocarbons.

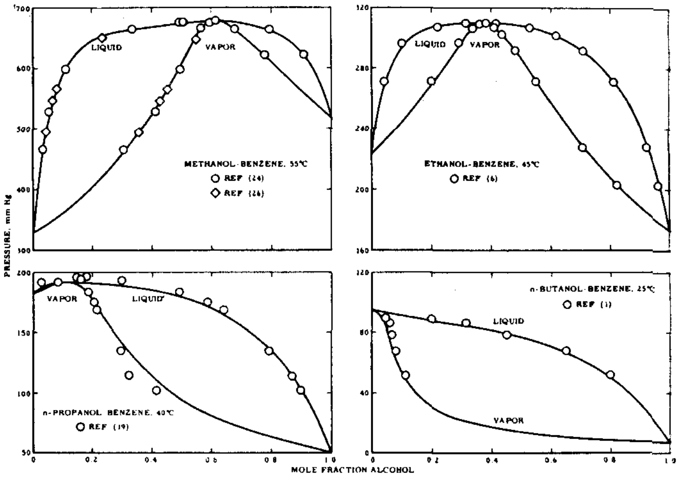

Fig. 17. Comparison of calculated and experimental vapor-liquid equilibria. (Lines are calculated.)

cients according to Equations (7), then use these to calculate the total pressure according to $P = \Sigma(\gamma_i x_i P_i^0/\theta_i)$. The vapor composition is calculated as $Y_1 = \gamma_1 x_1 P_1^0/\theta_1 P$. A trial calculation is used to establish final values for θ's starting with Y's calculated with the assumption that θ is unity.

Isobaric calculations are carried out by first making two isothermal calculations from which the boiling point at any liquid composition and prescribed total pressure is found by interpolating or extrapolating log P vs. $1/T$. Vapor-liquid equilibria are then calculated at each composition for which the boiling point was established.

Isothermal vapor-liquid equilibria calculated with the aid of the cross-correlated coefficients, Tables 2, 3, and 4, provide calculated results which can be compared directly with the original experimental values. One example for each of the eight binaries for which isothermal data are available is given in Figures 17 and 18.

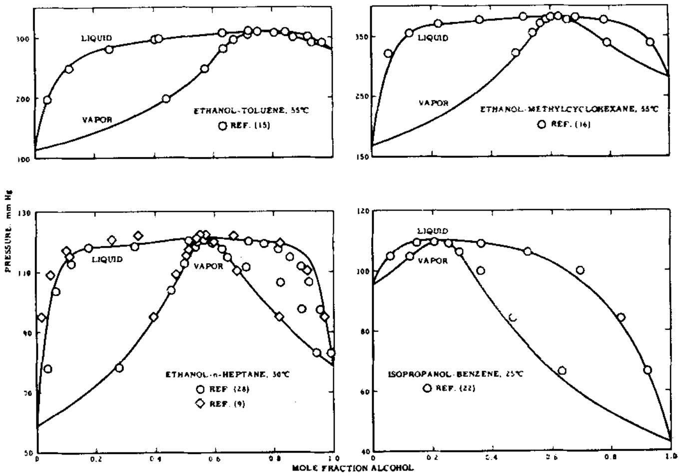

Fig. 18. Comparison of calculated and experimental vapor-liquid equilibria. (Lines are calculated.)

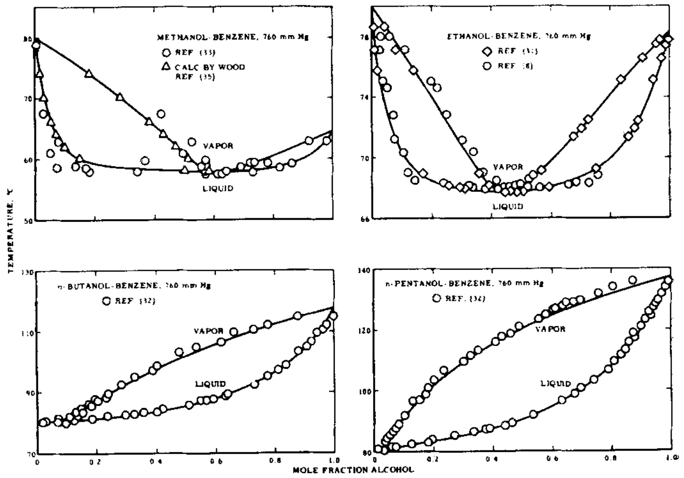

Fig. 19. Comparison of calculated and experimental vapor-liquid equilibria. (Lines are calculated.)

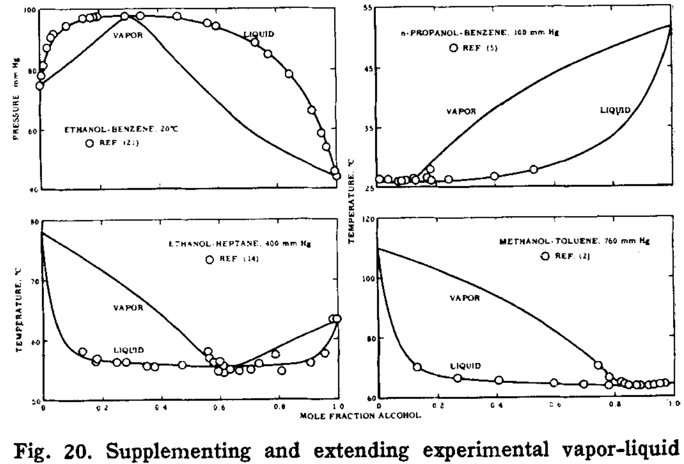

Fig. 20. Supplementing and extending experimental vapor-liquid equilibria. (Lines are calculated.)

In Figure 17 calculated and experimental vapor-liquid equilibria are compared for methanol-benzene at 55°C., ethanol-benzene at 45°C., *n*-propanol–benzene at 40°C., and *n*-butanol–benzene at 25°C. The excellent agreement is verification of the validity of Equations (2) and (7). The binaries represented best are the high-quality data of Scatchard and coworkers (*24*, *26*) and of Brown and Smith (*6*).

Calculated and experimental results are compared in Figure 18 for ethanol-toluene at 55°C., ethanol-methylcyclohexane at 55°C., ethanol-*n*-heptane at 30°C., and isopropanol-benzene at 25°C. The high-quality data of Kretchmer and coworkers (*15*, *16*) for the first two binaries are reproduced quite accurately by the calculations. The two sets of experimental data for ethanol–*n*-heptane are not in very good agreement with each other. For the binary isopropanol-benzene the coefficients used were those taken from the cross plots for the normal alcohols. The small deviations of the calculated from the observed results may be partly due to the effect of branching.

A few calculated isobaric vapor-liquid equilibria are compared with experimental data in Figure 19. For methanol-benzene at 760 mm. Hg the experimental data of Williams and coworkers (*33*) scatter markedly. The author's calculated results are in substantial agreement with the earlier calculations of Wood (*35*), as noted in the figure. Results calculated for ethanol-benzene at 760 mm. Hg are in good agreement with the experimental data of Wehe (*31*) and in rough agreement with the data of Drickamer and coworkers (*8*). Calculated results are in fair agreement with the data of Wehe (*32*) for *n*-butanol–benzene at 760 mm. Hg and the data of Arnold quoted by Wehe (*32*) for *n*-pentanol–benzene at the same pressure.

A basic advantage of the algebraic representation is realized when the data have been cross correlated as shown in Figures 1 to 4. Over the temperature range covered, isothermal vapor-liquid equilibria can be calculated with an accuracy sufficient for most practical purposes. In addition isobaric data at any desired pressure in the range of the correlations can also be derived. Incomplete data can be supplemented by calculations to furnish complete vapor-liquid equilibria; for example, Figure 20 shows four systems with incomplete experimental data which have been supplemented by calculations to furnish complete vapor-liquid equilibria.

In Figure 20 complete vapor-liquid equilibria calculated for ethanol-benzene at 20°C. are compared with the experimental total pressures of Niini (*21*). The partially complete data of Britton, *et al.* (*5*), for *n*-propanol–benzene at 100 mm. Hg and of Katz and Newman (*14*) for ethanol–*n*-heptane at 400 mm. Hg are compared with complete results provided from calculations. The nearly complete results of Benedict, *et al.* (*2*), are compared with vapor-liquid equilibria calculated for methanol-toluene at 760 mm. Hg.

As indicated in Figure 4 and confirmed in Figure 14, the estimated effect of temperature on the coefficients A_{12}, A_{21}, and c_{12} is about right for methanol-toluene. When one knows this, it is possible to calculate vapor-liquid equilibria at other temperatures and pressures. Accordingly vapor-liquid equilibria for this system at 9, 14.7, and 19.7 lb./sq. in. abs. have been predicted. Similarly vapor-liquid equilibria have been calculated for several isothermal and isobaric conditions for each of the alcohol-hydrocarbon binaries described here.*

Another advantage the cross-correlated coefficients provide is a means of predicting, with no additional data, the ternary or multicomponent vapor-liquid equilibria and heats of mixing in some of the mixtures. These are mixtures in which two of the three components in each ternary are of the same class, for example methanol and ethanol in ternary mixtures with benzene and benzene in multicomponent mixtures with the five alcohols. Ternary systems in which each of the three components is of a different class require data on all three binaries to calculate the ternary equilibria, for example, *n*-heptane–benzene–ethanol.

Accordingly, with the aid of Equations (12), (26), and (27) of reference (*4*), vapor-liquid equilibria have been calculated for benzene in three- to six-component mixtures with the normal chain alcohols methanol to *n*-pentanol. A simple ternary example, benzene–*n*-pentanol–ethanol at 14.7 lb./sq. in. abs. is given.*

In summary it has been shown that the modified van Laar type of equation provides an adequate representation of the effect of composition on the activity coefficient for binary mixtures of benzene and alcohols. Consequently these equations also furnish good values for the excess free energies. A cross correlation of the coefficients for these equations as a function of $1/T$ has been used to predict heats of mixing in good agreement with calorimetric data. From the excess free energies and the heats of mixing the excess entropy of solution has been obtained.

The consistent set of cross-correlated coefficients provides the basis for calculating both isothermal and isobaric vapor-liquid equilibria at various conditions for each of the binaries and for certain ternary and multicomponent mixtures without any additional data. The influences of carbon number of the alcohol and hydrocarbon type furnish a starting point for further extension of the results.

ACKNOWLEDGMENT

The author wishes to thank Emily King and Helen Taylor for assistance in making some of the calculations.

NOTATION

a_i = van der Waals' attraction constant for component i
b_i = van der Waals' covolume for component i
a_{ij}^2 = $A_{ij} - c_{ij}$ coefficients in Equations (7)
A_{ij} = common logarithm of the activity coefficient for component i at infinite dilution in liquid j
c_{ij} = coefficients in Equations (7)
E' and m = individual coefficients for calculating the molecular attraction coefficient for polar compounds
F_x^E = excess free energy/mole at composition x
$\overline{L}_{i_x}$ = differential heat of mixing/mole at composition x
H_x^M = integral heat of mixing/mole at composition x
n_c = carbon number
P = total pressure
P_i^0 = vapor pressure of pure component i
R = universal gas constant
S_x^E = excess entropy of mixing/mole at composition x
T = absolute temperature
t = boiling temperature
V_i' = approximation for molal volume of component i in liquid phase
x_i = mole fraction component i in liquid phase
x_E = mole fraction ethanol
Y_i = mole fraction component i in vapor phase

Greek Letters

γ_i = liquid phase activity coefficient for component i
θ_i = imperfection-pressure coefficient
ξ^0 = limiting value at zero pressure of the molecular attraction coefficient ξ
ξ^{*0} = nonpolar part of ξ^0
$\bar{\xi}^0$ = polar part of ξ^0
ξ_i = attraction coefficient
G_{ij} = $(a_i\xi_i{}^{*0})^{0.5} - (a_j\xi_j{}^{*0})^{0.5}$ and
$\overline{G}_{ij}$ = $(a_i\bar{\xi}_i{}^0)^{0.5} - (a_j\bar{\xi}_j{}^0)^{0.5}$, differences in the square roots of the nonpolar and polar parts, respectively, of the molal cohesive energies for components i and j
χ_i = constant in Equation (4)

LITERATURE CITED

1. Allen, B. B., S. P. Lingo, and W. A. Felsing, *J. Phys. Chem.*, **43**, 425 (1939).
2. Benedict, Manson, C. A. Johnson, E. Solomon, and L. C. Rubin, *Trans. Am. Inst. Chem. Engrs.*, **41**, 371 (1949).
3. Black, Cline, *Ind. Eng. Chem.*, **50**, 391 (1958).
4. *Ibid.*, p. 403.
5. Britton, E. C., H. S. Nutting, and L. H. Horsley, *Anal. Chem.*, **19**, 601 (1947).
6. Brown, I., and F. Smith, *Australian J. Chem.*, **7**, 264 (1954).
7. Chalela, D. A., H. H. Steinhauser, and J. O. Hougen, *Ind. Eng. Chem. Data Series*, **2**, 66 (1957).
8. Drickamer, H. G., G. G. Brown, and R. R. White, *Trans. Am. Inst. Chem. Engrs.*, **41**, 555 (1945).
9. Ferguson, J. B., M. Freed, and A. C. Morris, *J. Phys. Chem.*, **37**, 87 (1933).
10. Fiock, E. G., D. C. Ginnings, and W. B. Holton, *J. Research Natl. Bur. Standards*, **6**, 881 (1931).
11. Halford, J. O., *J. Chem. Phys.*, **17**, 111 (1949).
12. Ingle, J. D., and H. P. Cady, *J. Phys. Chem.*, **42**, 397 (1938).
13. Jones, L. H., and R. H. Badger, *J. Am. Chem. Soc.*, **73**, 3132 (1951).
14. Katz, Kurt, and Morris Newman, *Ind. Eng. Chem.*, **48**, 137 (1956).
15. Kretchmer, C. B., and Richard Wiebe, *J. Am. Chem. Soc.*, **71**, 1793 (1949).
16. ———, *Ibid.*, p. 3176.
17. ———, *Ibid.*, **76**, 2579 (1954).
18. Lambert, J. D., G. A. H. Roberts, J. S. Rowlinson, and V. J. Wilkinson *Proc. Roy. Soc.* (*London*), **A196**, 113 (1949).
19. Lee, Siang Chah., *J. Phys. Chem.*, **35**, 3558 (1931).
20. Niini, A., *Ann. Acad. Sci. Fennicae*, **A55**, No. 8, 1 (1940).
21. ———, *Suomalainen Tiedeakat. Toimituksia A. 55* (1940).
22. Olsen, A. L., and E. R. Washburn, *J. Phys. Chem.*, **41**, 457 (1937).
23. Rowlinson, J. S., *Trans. Faraday Soc.*, **45**, 974 (1949).
24. Scatchard, George, S. E. Wood, and J. H. Mochel, *J. Am. Chem. Soc.*, **68**, 1957 (1946).
25. Scatchard, George, L. B. Ticknor, J. R. Goates, and E. R. McCartney, *ibid.*, **74**, 3721 (1952).
26. Scatchard, George, and L. B. Ticknor, *ibid.*, p. 3724.
27. Schmidt, G. C., *Z. physik. Chem.*, **121**, 221 (1925).
28. Smyth, C. P., and E. W. Engel, *J. Am. Chem. Soc.*, **51**, 2260 (1929).
29. Tsao, C. C., and J. M. Smith, *Chem. Eng. Progr. Symposium Ser. 7*, **49**, 107 (1953).
30. Washburn, E. R., and A. Lightbody, *J. Phys. Chem.*, **34**, 2701 (1930).
31. Wehe, A. H., *A.I.Ch.E. Journal*, **1**, 24 (1955).
32. ———, *ibid.*; refers to private communication from T. H. Arnold.
33. Williams, G. C., S. Rosenberg, and H. A. Rothenberg, *Ind. Eng. Chem.*, **40**, 1273 (1948).
34. Wolfe, K. L., H. Behlke, and K. Wehage, *Z. physik. Chem.*, **B28**, 1 (1935).
35. Wood, S. E., *Ind. Eng. Chem.*, **42**, 660 (1950).

Manuscript received June 23, 1958; revision received October 31, 1958; paper accepted November 26, 1958. Paper presented at A.I.Ch.E. Salt Lake City meeting.

---

*See footnote p. 249.